Instability of nonplanar modulated dust acoustic wave packets in a strongly coupled nonthermal dusty plasma

Article *in* Physics of Plasmas · July 2015

Impact Factor: 2.14 · DOI: 10.1063/1.4923433

3 authors, including:

Salah Kamel El-Labany
Damietta University
101 PUBLICATIONS **1,196** CITATIONS

SEE PROFILE

Wael Farouk El-Taibany
Damietta University
62 PUBLICATIONS **1,410** CITATIONS

SEE PROFILE

Instability of nonplanar modulated dust acoustic wave packets in a strongly coupled nonthermal dusty plasma

S. K. El-Labany, W. F. El-Taibany, and N. A. Zedan

Citation: Physics of Plasmas **22**, 073702 (2015); doi: 10.1063/1.4923433
View online: http://dx.doi.org/10.1063/1.4923433
View Table of Contents: http://scitation.aip.org/content/aip/journal/pop/22/7?ver=pdfcov
Published by the AIP Publishing

Instability of nonplanar modulated dust acoustic wave packets in a strongly coupled nonthermal dusty plasma

S. K. El-Labany,[1,a)] W. F. El-Taibany,[1,2,b)] and N. A. Zedan[1,c)]
[1]*Department of Physics, Faculty of Science, Damietta University, New Damietta, P.O. 34517, Egypt*
[2]*Department of Physics, College of Science for Girls in Abha, King Khalid University, P.O. 960 Abha, Kingdom of Saudi Arabia*

(Received 1 April 2015; accepted 15 June 2015; published online 9 July 2015)

Cylindrical and spherical amplitude modulations of dust acoustic (DA) solitary wave envelopes in a strongly coupled dusty plasma containing nonthermal distributed ions are studied. Employing a reductive perturbation technique, a modified nonlinear Schrödinger equation including the geometrical effect is derived. The influences of nonthermal ions, polarization force, and the geometries on the modulational instability conditions are analyzed and the possible rogue wave structures are discussed in detail. It is found that the spherical DA waves are more structurally stable to perturbations than the cylindrical ones. Possible applications of these theoretical findings are briefly discussed. © *2015 AIP Publishing LLC*. [http://dx.doi.org/10.1063/1.4923433]

I. INTRODUCTION

Dust contaminated plasmas have recently received a considerable interest due to their wide occurrence in real charged particle systems, both in space and laboratory, and to the novel physics involved in their description.[1] An issue of particular interest is the existence of special acoustic-like oscillatory modes; one of these important modes is the dust acoustic (DA) wave which was theoretically predicted[2] and later experimentally confirmed.[3]

Theoretically, the nonlinear solitary waves in plasma can be described by either the Korteweg de Vries (KdV) equation or the nonlinear Schrödinger equation (NLSE). The KdV equation describes the evolution of a non-modulated wave, i.e., a bare pulse with no fast oscillations inside the wave packet which is usually called the KdV soliton. The NLSE governs the dynamics of a modulated wave packet.

The modulational instability (MI) is a generic nonlinear phenomenon governing nonlinear wave propagation in dispersive media. It refers to weak space-time dependence (modulation) of the wave amplitude, due to intrinsic medium nonlinearity, however, weak. Under the effect of external perturbations, the amplitude of the wave envelope may potentially grow, eventually leading to energy localization via the formation of localized structures (envelope solitons).[4] The physics of soliton creation/propagation produced from KdV and NLSE are significantly different.[5] It is well known that nonlinear wave propagation is generically subject to the modulation due to the carrier wave self-interaction. Recently, the MI of DA waves and their propagations in dusty plasma have received a considerable attention[5–8] because of their relevance to certain observations in space and laboratory plasmas. However, most considerations of the modulated waves in dusty plasmas are limited to planar geometry. The unbounded planar geometry may not be a realistic situation in laboratory devices and space. Moreover, various studies[9–11] show that the properties of solitary waves in nonplanar cylindrical/spherical geometry are different from those of planar geometry. Though, most of these investigations concern with the KdV equation. Franz *et al.*[12] have shown that a purely one-dimensional model cannot account for all observed features in the auroral region, especially at higher polar altitudes. Meanwhile, the waves observed in laboratory devices are certainly not bounded in a one dimension, but usually in multi-dimension geometry. On the other side, the MI studies[5,13–15] of the DA waves were mainly focused on Maxwellian distribution. Whereas, the space plasma observations, for example, in the Earth's bow-shock, in the upper ionosphere of Mars, and in the vicinity of Moon,[16] clearly indicate the presence of ions and electrons whose distributions depart from the Maxwellian distribution. Therefore, a great deal of attention has been paid to non-Maxwellian distributions. The effects of nonthermal ion distributions on nonlinear DA wave propagation in unmagnetized[17] and magnetized[18] plasma have been reported. They found the possibility of creating both of rarefactive and compressive DA solitary waves in these plasma models.[17,18] Later on, MI of DA waves in dusty plasma including nonthermal ions is investigated[19] revealing that the condition of the MI is modified due to the presence of nonthermal ions.

On the other hand, the dusty plasma could be in a strongly coupled state because the interaction energy of neighbouring dust particles due to shielded Coulomb force is much larger than their thermal energy.[20] The coupling between particles can be depicted from the screened Coulomb coupling parameter: $\Gamma_s[=\left(\frac{q_d^2}{a_d T_d}\right)\exp\left(-\frac{a_d}{\lambda_D}\right)]$, where q_d is the dust grain charge, a_d is the intergrain distance, T_d is the dust temperature, and λ_D is the dusty plasma Debye radius] is comparable to unity or even much larger than one; $\Gamma_s \gg 1$. Later on, there are a number of investigations focusing on studying a strongly coupled dusty plasma

[a)]Email: skellabany@hotmail.com.
[b)]Author to whom correspondence should be addressed. Electronic addresses: eltaibany@hotmail.com and eltaibany@du.edu.eg.
[c)]Email: nesreenplasma@yahoo.com.

(SCDP) both theoretically and experimentally.[21–26] The linear analyses[21] have revealed that strong correlations introduce modifications to the DA wave modes such as new dispersion corrections and additional damping effects. On the other side, the nonlinear analyses produce new salient features for the DA solitary waves.[22–26] For example, the DA solitary and shock waves are found to exist with negative potential only in a SCDP including nonthermal ions and Boltzmann distributed electrons.[22] The effect of the polarization force on the propagation of linear and nonlinear DA waves has been considered by Mamun and his coworkers[23] in different SCDP models. These studies reveal that the phase speed of the DA waves, as well as the dust density perturbation, increase (decrease) with the increase of nonthermal ions (polarization force), and that the potential associated with the DA waves decreases with the increase of the equilibrium dust number density. El-Labany *et al.*[24] introduced the first study of head-on-collision of two modulated DA wave envelope solitons in SCDP within the NLSE framework in both of hydrodynamic and kinetic regimes. Since the polarization effects are included in their models, they considered only Maxwellian distributed species and planar geometry. Recently, including the nonplanar geometrical effect along with the polarization force in studying DA solitary waves in SCDP models explores significant new features.[25,26]

Up to the best of our knowledge, the effects of nonplanar (cylindrical and spherical) geometries as well as the polarization force effect on the amplitude modulation DA envelope solitary waves with nonthermal distributed ions have not been investigated yet. Therefore, this is the main aim of this manuscript by assuming a three-components SCDP consisting of negatively charged dust grains, nonthermal ions and Maxwellian electrons. Here, the dust grains are assumed to have constant dust charge since the charging time is much shorter than the DA dynamical time as detected in recent experiment and proved theoretically.[27] Therefore, in this paper, we shall study the MI of DA wave envelopes in cylindrical and spherical geometries in the framework of the modified NLSE.

The paper is organized in the following fashion: In Sec. II, we present the relevant equations governing the dynamics of nonlinear DA waves. Accounting for the nonthermal ion distribution function and introducing a reductive perturbation technique (RPT), a modified NLSE is derived. In Sec. III, the possible rational solutions of the modified NLSE are analyzed. In Sec. IV, we discuss the MI criterion of the DA wave envelopes in nonplanar geometries. Section V presents a set of numerical illustrations and results discussion then finally the conclusion is provided.

II. DERIVATION OF THE MODIFIED NLSE

We consider the nonlinear propagation of DA waves[2,18,22] in a SCDP whose constituents are electrons, nonthermal ions, and negatively charged dust grains. At equilibrium, we have $n_{io} = n_{eo} + Z_d n_{do}$, where n_{io} (n_{eo}) n_{do} is the equilibrium ion (electron) dust number density and Z_d is the number of electrons residing on the dust grain surface. Compared to the dust grains, we assume that electrons and ions are weakly coupled due to their higher temperatures and smaller electric charges, though dust grains are strongly coupled due to their lower temperature and larger electric charge.[18,22]

As we are concerned in the present study with the DA low frequency solitary wave modes, it is recognized that the dust dynamical time scale is larger than of both of ion and electron species. In addition, the latter is the fastest species in this model, so it could reach the thermal equilibrium quicker than others and it obeys the Maxwellian distribution. Therefore, the electron distribution is given by $n_e = n_{eo}\exp\left(\frac{e\varphi}{T_e}\right)$, whereas the ions, obeying the nonthermal distribution function, and its number density is given by $n_i = n_{io}\left[1 + \frac{e\beta\varphi}{T_i} + \beta\left(\frac{e\varphi}{T_i}\right)^2\right]e^{-\frac{e\varphi}{T_i}}$, where $\beta = \frac{4\alpha}{1+3\alpha}$ with α being a parameter which determines the population of nonthermal ions in our plasma model.[18,19,22,23,28]

One of the main motives of the present study is to examine the polarization force effects on the time-dependent nonlinear and nonplanar DA wave structures. The polarization force (F_p) acting on a dust grain is defined as[22,25,29] $F_P = -Z_d e\tilde{R}(n_i/n_{io})^{1/2}\nabla\varphi$, where $\tilde{R} = Z_d e^2/(4T_i\lambda_{Dio})$ is a parameter determining the effect of the polarization force and $\lambda_{Dio} = [T_i/(4\pi e^2 n_{io})]^{1/2}$. The summation of the electric force ($F_e = Z_d e\nabla\varphi$) and the polarization force, F_P, can be expressed in nonplanar (cylindrical or spherical) coordinates as[22,25]

$$F_r = Z_d e[1 - \tilde{R}(n_i/n_{io})^{1/2}](\partial\varphi/\partial r).$$

The dynamics of the nonlinear DA wave envelopes in such a SCDP are governed by the generalized hydrodynamics normalized equations[21,30,31]

$$\frac{\partial n_d}{\partial t} + \frac{1}{r^\nu}\frac{\partial(r^\nu n_d u_d)}{\partial r} = 0, \tag{1}$$

$$n_d\left[\frac{\partial u_d}{\partial t} + u_d\frac{\partial u_d}{\partial r} - \left(1 - R\sqrt{n_i}\right)\frac{\partial\varphi}{\partial r} + \sigma_d\mu_d\frac{1}{n_d}\frac{\partial n_d}{\partial r}\right] = \frac{\eta}{r^\nu}\frac{\partial}{\partial r}\left(r^\nu\frac{\partial u_d}{\partial r}\right) + \eta_L\frac{\partial}{\partial r}\left[\frac{1}{r^\nu}\frac{\partial}{\partial r}(r^\nu u_d)\right], \tag{2}$$

$$\frac{1}{r^\nu}\frac{\partial}{\partial r}\left(r^\nu\frac{\partial\varphi}{\partial r}\right) = \mu_e e^{\sigma_i\varphi} - \mu_i\left(1 + \beta\varphi + \beta\varphi^2\right)e^{-\varphi} + n_d, \tag{3}$$

where $\nu = 0$ corresponds to a 1D-planar geometry and $\nu = 1$ (2) is for a nonplanar cylindrical (spherical) geometry. $n_d(u_d)$ is the dust number density (dust fluid velocity). t (r) is time (space) variable and $R = \tilde{R}/\sqrt{\mu_i}$ and μ_d is the compressibility. In the present model, we focus our study to a SCDP in the hydrodynamic regime where $\omega\tau_m \ll 1$ with τ_m is viscoelastic relaxation time. Moreover, we consider the viscosity contribution [$\eta(\zeta)$ is the bulk (shear) viscosity coefficient, and $\eta_L = \zeta + (\eta/3)$ is the longitudinal viscosity coefficient] is small compared to the compressibility contribution.[24] As discussed in Refs. 21 and 24, simulation and model calculations typically show that $\eta_L \sim 0.08$ for

$\Gamma_s \sim 10$, whereas $\mu_d \sim 1$ in that region. Hence, we can neglect the viscous dissipation effect by a suitable choice of ordering. It is noted that there are various approaches for calculating these transport coefficients appeared in Eq. (2) which have been widely discussed in the literature.[21,32–34]

The physical parameters presented in Eqs. (1)–(3) are normalized as: time t, radial distance r, n_d, u_d, η_L, and the electrostatic potential φ are normalized by the reciprocal dust plasma frequency ω_{pd}^{-1} $(\omega_{pd} = \sqrt{4\pi(Z_d e)^2 n_{do}/m_d})$, Debye radius $\lambda_{Di}[= \sqrt{T_i/(4\pi Z_d e^2 n_{do})}]$, n_{do}, $C_d(= \sqrt{Z_d T_i/m_d})$, $m_d n_{do}\omega_{pd}\lambda_{Di}^2$ and T_i/e, respectively. We use the parameters $\mu_e = \frac{n_{eo}}{Z_d n_{do}}$, $\mu_i = \frac{n_{io}}{Z_d n_{do}}$, $\sigma_i = \frac{T_i}{T_e}$, and $\sigma_d = \frac{T_d}{Z_d T_i}$ where the other parameters have their normal definitions.

In order to investigate the amplitude modulation of DA envelope solitary waves in our SCDP system, we employ the reductive perturbation technique.[35] In this technique, the independent variables are stretched as $\xi = \epsilon(r - \lambda t)$ and $\tau = \epsilon^2 t$, where ϵ is a small (real) parameter and λ is the envelope group velocity to be determined later and the dependent variables are expanded as

$$\tilde{\Gamma}(r,t) = \tilde{\Gamma}_0 + \sum_{m=1}^{\infty} \epsilon^m \sum_{L=-\infty}^{\infty} \tilde{\Gamma}_L^{(m)}(\xi,\tau)\exp(iL\theta), \quad (4)$$

where $\tilde{\Gamma}_L^{(m)} = [\mathrm{n}_{dL}^{(m)} u_{dL}^{(m)} \varphi_L^{(m)}]^T$, $\tilde{\Gamma}_L^{(0)} = [1 \;\; 0 \;\; 0]^T$, $\theta = kr - \omega t$, k and ω are real variables representing the fundamental (carrier) wave number and frequency, respectively. All elements of $\tilde{\Gamma}_L^{(m)}$ satisfy the reality condition $\tilde{\Gamma}_{-L}^{(m)} = \tilde{\Gamma}_L^{*(m)}$, where the asterisk denotes the complex conjugate. Substituting Eq. (4) into Eqs. (1)–(3), we get a set of reduced equations. Collecting terms of the same powers of ϵ, we have for the first-order $(m = 1)$ equations with $L = 1$, $n_{d1}^{(1)} = \alpha_n \varphi_1^{(1)}$, $u_{d1}^{(1)} = \frac{\alpha_n \omega}{k}\varphi_1^{(1)}$ where $\alpha_n = -(k^2 + \gamma)$, $\gamma = \mu_e\sigma_i + \mu_i\left(1 - \frac{4\alpha}{1+3\alpha}\right)$ and the dispersion relation is

$$\omega = k\sqrt{\left(\sigma_d\mu_d + \frac{R-1}{\alpha_n}\right)}. \quad (5)$$

The second-order $(m = 2)$ reduced equations with $L = 1$ are given by

$$\left.\begin{aligned} i\xi\left(-\omega n_{d1}^{(1)} + k u_{d1}^{(1)}\right) + i\lambda\tau\left(-\omega n_{d1}^{(2)} + k u_{d1}^{(2)}\right) &= \lambda^2\tau\frac{\partial n_{d1}^{(1)}}{\partial\xi} - \lambda\tau\frac{\partial u_{d1}^{(1)}}{\partial\xi}, \\ -i\omega u_{d1}^{(2)} + ik\sigma_d\mu_d n_{d1}^{(2)} - ik(1-R)\varphi_1^{(2)} &= \lambda\frac{\partial u_{d1}^{(1)}}{\partial\xi} + (1-R)\frac{\partial\varphi_1^{(1)}}{\partial\xi} - \sigma_d\mu_d\frac{\partial n_{d1}^{(1)}}{\partial\xi}, \\ \frac{\xi}{\lambda\tau}\left(-\alpha_n\varphi_1^{(1)} + n_{d1}^{(1)}\right) - \alpha_n\varphi_1^{(2)} + n_{d1}^{(2)} &= 2ik\frac{\partial\varphi_1^{(1)}}{\partial\xi}. \end{aligned}\right\} \quad (6)$$

Solving this system of equations with the help of the first-order quantities and Eq. (5), we can express the second-order quantities with L = 1 as

$$n_{d1}^{(2)} = \alpha_n\varphi_1^{(2)} + 2ik\frac{\partial\varphi_1^{(1)}}{\partial\xi}, \quad (7)$$

$$u_{d1}^{(2)} = \frac{\alpha_n\omega}{k}\varphi_1^{(2)} + i\left[2\omega - \frac{\lambda\alpha_n}{k} + \frac{\alpha_n\omega}{k^2}\right]\frac{\partial\varphi_1^{(1)}}{\partial\xi}, \quad (8)$$

and Poisson's equation leads to the compatibility condition

$$\lambda = \frac{\partial\omega}{\partial k} = \left(\frac{k}{\omega}\right)\left[\sigma_d\mu_d + \frac{\gamma(1-R)}{(\gamma+k^2)^2}\right], \quad (9)$$

which determines the group velocity of the DA wave envelope in the present SCDP. Going further in the perturbation theory, we get the second harmonic modes (L = 2) arising from the nonlinear self-interaction of the carrier waves which are calculated in terms of $[\varphi_1^{(1)}]^2$ as

$$(n_{d2}^{(2)} \;\; \varphi_2^{(2)} \;\; u_{d2}^{(2)})^T = (N_1 \;\; N_{23} \;\; N_4)^T [\varphi_1^{(1)}]^2, \quad (10)$$

where $N_a, a = 1, 2, 3, 4$ are given in the Appendix.

In addition, the nonlinear self-interaction of the carrier wave yields to the creation of a zeroth-order harmonic. Its strength is analytically determined by taking $L = 0$ component of the third-order reduced equations and they can be expressed as

$$(n_{d0}^{(2)} \;\; u_{d0}^{(2)} \;\; \varphi_0^{(2)})^T = (N_5 \;\; N_6 \;\; N_{78})^T |\varphi_1^{(1)}|^2, \quad (11)$$

where $N_b, b = 5, 6, 7, 8$ are given in the Appendix.

Finally, the third-order perturbed equations and the first harmonic modes, with the aid of Eqs. (10) and (11), give a system of equations. By solving the latter system of equations, we get the following modified NLSE:

$$i\frac{\partial\phi}{\partial\tau} + P\frac{\partial^2\phi}{\partial\xi^2} + Q|\phi|^2\phi + i\frac{\nu}{2\tau}\phi = 0, \quad (12)$$

where $\phi \equiv \varphi_1^{(1)}$ is set for simplicity. The term $i(\nu/2\tau)\phi$ in Eq. (12) accounts for the geometric effects. In Eq. (12), the dispersion coefficient, P, reads

$$P = \frac{1}{2}\frac{\partial^2\omega}{\partial k^2} = \frac{a_7 k}{2\alpha_n\omega} + \frac{a_2}{2\lambda\tau\alpha_n} + \frac{k^2(1-R)}{2\alpha_n\omega(\gamma+k^2)}, \quad (13)$$

and the nonlinear coefficient, Q, is

$$Q = \frac{a_9 k}{2\alpha_n \omega} + \frac{a_4}{2\lambda\tau\alpha_n} + \frac{a_6 k^2(1-R)}{2\alpha_n\omega(\gamma + k^2)}, \quad (14)$$

where a_i, $i = 1, \ldots, 9$ are given in the Appendix.

III. RATIONAL SOLUTIONS OF THE NLSE

First, we have to note that an exact analytic solution of the modified NLSE, (12) is not possible[19,26,36] except for some cases where the inverse scattering transformation method can be applied. On the other side, for $\nu = 0$, the focusing of NLSE (12) has a variety of solutions, among them there is a hierarchy of rational solutions that are localized in both ξ and τ variables. Each solution of the hierarchy represents a unique event in space and time, as it increases its amplitude quickly along each variable, reaching its maximum value and suddenly disappears, just as quickly as it appeared.[37] Thus, these waves have the property *"waves that appear from nowhere and disappear without a trace"*[38] and they are named *"rogue waves."* The rogue wave is a non-stationary solution[39] and it is usually an envelope of a carrier wave with a wavelength smaller than the central region of the envelope. Using the Darboux transformation method, Akhmediev and his co-workers[37–41] have derived the rational rogue wave solution of the NLSE. The most convenient way to write each rational solution is[37,38,41,42]

$$\psi_j(\xi,\bar{\tau}) = \psi_o\left[(-1)^j + \frac{G_j(\xi,\bar{\tau}) + i\bar{\tau}H_j(\xi,\bar{\tau})}{F_j(\xi,\bar{\tau})}\right]\exp(i\bar{\tau}), \quad (15)$$

where ψ_o is the background amplitude, $\bar{\tau} = P\tau$; and j being the order of the solution ($j \geq 1$). Here, $G_j(\xi,\bar{\tau}), H_j(\xi,\bar{\tau})$ and $F_j(\xi,\bar{\tau})$ are polynomials in the variables ξ and, $\bar{\tau}$, and $F_j(\xi,\bar{\tau})$ has no real zeros. Higher order solutions are progressively more complicated,[41] therefore, we will concern our study with the cases $j \leq 2$. It may be remarked that to get the details of deriving the NLSE rational solution, (15), using the Darboux transformation method, please consult Ref. 41.

For the first-order/fundamental rogue wave solution; $j = 1$, we have[38]

$$H_1(\xi,\bar{\tau}) = 2G_1(\xi,\bar{\tau}) = 8 \text{ and } F_1(\xi,\bar{\tau}) = 1 + 4(\xi^2 + \bar{\tau}^2), \quad (16)$$

this solution is known as the *Peregrine soliton,* in honour of the first person who showed that such solution could be the prototype of rogue waves in the ocean.[43] This solution is localized in space and time and the maximal amplitude amplification obtained at $\xi = 0$ and $\bar{\tau} = 0$ is three times the height of the carrier wave.

The second order/super rogue wave solution; $j = 2$, the polynomials for this solution are given by[41,44]

$$H_2(\xi,\bar{\tau}) = \frac{15}{4} + 2\xi^2(3 - 2\xi^2) - 2\bar{\tau}^2(1 + 4\xi^2 + 2\bar{\tau}^2) \quad (17)$$

$$G_2(\xi,\bar{\tau}) = \frac{3}{8} - \xi^2(3 + 2\xi^2) - \bar{\tau}^2(9 + 12\xi^2 + 10\bar{\tau}^2), \quad (18)$$

and

$$F_2(\xi,\bar{\tau}) = \frac{1}{8}\left\{\frac{3}{4} + \xi^2\left(9 + 4\xi^2 + \frac{16}{3}\xi^4\right) + \bar{\tau}^2\left(33 + 36\bar{\tau}^2 + \frac{16}{3}\bar{\tau}^4\right) + 8(\bar{\tau}\xi)^2\left[-3 + 2\left(\xi^2 + \bar{\tau}^2\right)\right]\right\}. \quad (19)$$

The solution (15) represents the profile of the rogue wave within the modulational unstable region, which concentrates a significant amount of energy into a relatively small area, and therefore rogue waves are generated in our plasma. This property of the nonlinear solution may serve as the basis for the explanation of the DA waves in a SCDP. The second-order solution $|\psi_2(\xi,0)|$ and the first-order solution $|\psi_1(\xi,0)|$ have, respectively, four and two zeros symmetrically located on the ξ axis. Thus, the solutions $|\psi_2(\xi,0)|$ and $|\psi_1(\xi,0)|$ have three and one local maxima, respectively.[41]

Recently, Chabehoub *et al.*[44] found that the experimental and theoretical values of the amplification in the water-wave tank for the second-order solution are very close to excellent. Also, they found that the super rogue waves ψ_2 may be more real than the first one (ψ_1) in fields concerned with nonlinear dispersive media, e.g., in optics, plasma physics, and superfluidity. Furthermore, Guo *et al.*[45] studied the nonlinear propagation of planar ion-acoustic rogue waves (IARWs) in an unmagnetized electron-positron-ion dust plasma. They investigated the influence of the plasma parameters on the nonlinear structures of the first-and second-order IARW solutions within the modulational unstability region. From the present study, it is clear that the deviation from Maxwellian state would lead to appearance of new characteristics that should be taken into account during the future experiments.

IV. MI OF SPHERICAL AND CYLINDRICAL DA WAVE EXCITATIONS

Since the rogue wave solution appears at the unstable domain for the nonlinear DA wave packets, it is important in this section to investigate the MI of these nonplanar wave excitations, following the analysis of Jukui and Lang[46] that is summarized below. The development of the small modulation $\delta\phi$ is investigated according to

$$\phi = \left[\bar{\phi}_o + \delta\phi(\xi,\tau)\right]\exp\left[-i\int_{\tau_o}^{\tau}\Delta(\tau')d\tau' - \frac{\nu}{2}\ln\tau\right], \quad (20)$$

where $\bar{\phi}_o$ is the constant (real) amplitude of the pump carrier wave and Δ is a nonlinear frequency shift. Suppose the perturbation $\delta\phi$ is defined as

$$\delta\phi = \delta\bar{\phi}_o \exp\left\{i\left[K\xi - \int_{\tau_o}^{\tau}\Omega(\tau')d\tau'\right]\right\} + c.c., \quad (21)$$

where $K\xi - \int_{\tau_o}^{\tau}\Omega d\tau'$ is the modulation phase with K and Ω is the perturbation wave number and the frequency of the wave

modulation, respectively.[36,46] Using Eqs. (20) and (21) in NLSE, one obtains the nonlinear dispersion relation

$$\Omega(\tau) = PK^2\sqrt{1 - \frac{2Q\,|\bar{\phi}_o|^2}{PK^2\tau^\nu}}, \tag{22}$$

which exactly reduces to the nonlinear dispersion relation for planar geometry when $\nu = 0$.[47] We immediately see that the MI condition will be satisfied if $PQ > 0$ and $K^2 \le K_c^2(\tau) = 2Q\,|\bar{\phi}_o|^2/(P\tau^\nu)$. The local instability growth rate, for $\nu \neq 0$, is given by

$$Im\,\Omega(\tau) = PK^2\sqrt{[K_c(\tau)/K]^2 - 1}. \tag{23}$$

The instability growth rate will cease for cylindrical geometry ($\nu = 1$) when

$$\tau \ge \tau_{max} = \frac{2|\bar{\phi}_o|^2}{K^2}\frac{Q}{P}, \tag{24}$$

whereas for spherical geometry ($\nu = 2$), it becomes

$$\tau \ge \tau_{max} = \frac{|\bar{\phi}_o|}{K}\sqrt{\frac{2Q}{P}}. \tag{25}$$

It is clear that there is a MI period, τ, for cylindrical and spherical wave modulation, which does not exist in the one-dimensional planar case. The total growth rate (Γ) of the modulation during the unstable period is[46]

$$\Gamma = \exp\left(\int_{\tau_0}^{\tau_{max}} Im\,\Omega\,d\tau'\right) = \exp\left[\frac{Q|\bar{\phi}_o|^2}{\tau^{\nu-1}}f(R')\right], \tag{26}$$

where $R' = [2Q|\bar{\phi}_o|^2/PK^2\tau_0^\nu)] \ge 1$. For cylindrical geometry, we have

$$f(R') = f_{cyl} = \arctan\sqrt{R'-1} - \frac{\sqrt{R'-1}}{R'}, \tag{27}$$

while for spherical geometry,

$$f(R') = f_{sph} = \frac{1}{\sqrt{R'}}\ln\left(\frac{\sqrt{R'}+\sqrt{R'-1}}{\sqrt{R'}-\sqrt{R'-1}}\right) - \frac{2\sqrt{R'-1}}{R'}. \tag{28}$$

We note that f_{cyl} is an increasing function in R', and $f_{cyl} \to \pi/2$ as $R' \to \infty$. This means that during the MI period, the total growth increases as R' does for the cylindrical case. But, for f_{sph}, it has a maximum value given by

$$max\,f_{sph} = 2\sqrt{R_c - 1}/R_c, \tag{29}$$

where R_c is determined from $\sqrt{\frac{R_c}{R_c-1}}\ln\left(\frac{\sqrt{R_c}+\sqrt{R_c-1}}{\sqrt{R_c}-\sqrt{R_c-1}}\right) = 4$.

For spherical geometry, the MI growth rate will achieve its maximum at $R' = R_c$ and then decreases as R' increases further. It should be remarked that the MI period given by Eq. (24) for cylindrical geometry is longer than that determined by Eq. (25) for spherical geometry; meanwhile, during the unstable period, the MI growth rate is always an increasing function of R' in the cylindrical geometry, but not in the spherical geometry. This suggests that the spherical waves are more structurally stable to perturbations than the cylindrical waves.

V. NUMERICAL ILLUSTRATIONS, DISCUSSIONS AND CONCLUSIONS

We have derived a modified NLSE, (12), which includes a damping term that accounts for the geometric effect using a RPT for an unmagnetized SCDP containing negative dust grains, Maxwellian electrons and incorporating the effects of nonthermal ions.

Physically, both phase and group velocities of the DA wave are modified by the plasma parameter changes. This essentially entails a modification in the dispersive and nonlinear behavior of the DA plasma wave, which is manifested in the wavepacket's modulational profile. It is remarked here that the present results agree exactly with those of Ref. 48 by setting $\beta = 0$, i.e., by omitting the deviation from Maxwellian ion distribution. Also, they are in a good agreement with Ref. 24 by putting $\beta = 0$ and $\nu = 0$.

The effects of different physical parameters on the envelope dynamics will be investigated in terms of relevant parameters, namely, (i) the wave number k, (ii) the polarization parameter R, and, (iii) the value of the nonthermality ion parameter β, and (iv) the geometric effect, ν. Figure 1 shows that increasing the ion nonthermality characters leads to an increasing of the wave angular frequency, ω. The group velocity, λ firstly increases as β increase for long wavelengths (small/moderate values of wavenumbers; k). Though, at large wavenumber values ($k > 0.75$), this response is reversed. Moreover, increasing R yields to decrease of both of ω and λ which agrees with the previous studies focused on the polarization force effects.[23] The variations of the dispersion [nonlinear] coefficient, P [Q], appeared in the NLSE, Eq. (12), are investigated in Fig. 2 against β and R changes. Figure 2(a) proves that P is always negative[4,26] though Q [Fig. 2(b)] changes from positive to negative values. Since the product PQ plays a significant role in determining stable/unstable domain for DA wave propagation, we devote Fig. 3 to determine these regions. Figure 2 elucidates that increasing β leads to an increase of the wave dispersion, P, though it decreases the nonlinear effect, Q. On the other side, as R increases, both of P and Q decrease. Figure 3 investigates the existence of two stable domains separated by one unstable region for DA wave propagation. It is obvious that for very small values of k (long wavelengths), the DA wave is stable. Since increasing R results as shrink of both the two stable domains. In other words, including the polarization effects extends the unstable region. In addition, the effect of increasing β is just a slight increment of the lower stable domain, though it reduces the other higher stable domain. The variation of the threshold critical wave number, K_c, in different geometries and for different values of β, and $\sigma_i(= T_i/T_e)$ is shown in Fig. 4. In general, K_c decreases as k increases whatever the considered geometry. It is also seen that as β increases K_c decreases while the opposite response is observed by increasing σ_i. The lower (higher) critical wave number belongs to the spherical (cylindrical) geometry. For nonplanar

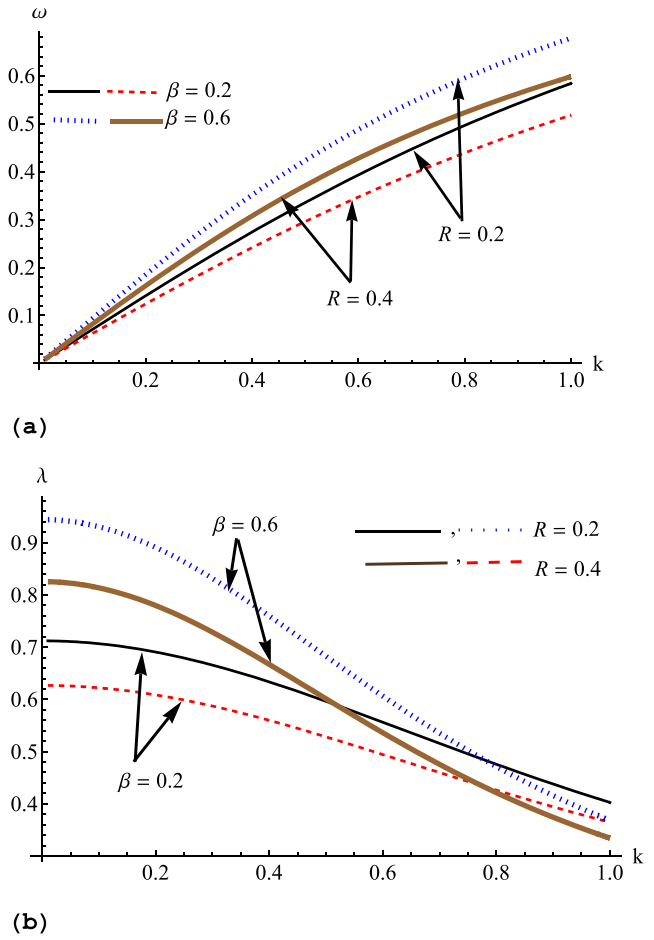

FIG. 1. Variation of the wave frequency, ω [group velocity, λ] in panel (a) [(b)], respectively, against the wave number k for different values of the nonthermality (polarization) parameter, β (R) where $\sigma_i = 0.15$, $\sigma_d = 0.05$, $\mu_i = 2.33$, and $\mu_e = 1.33$.

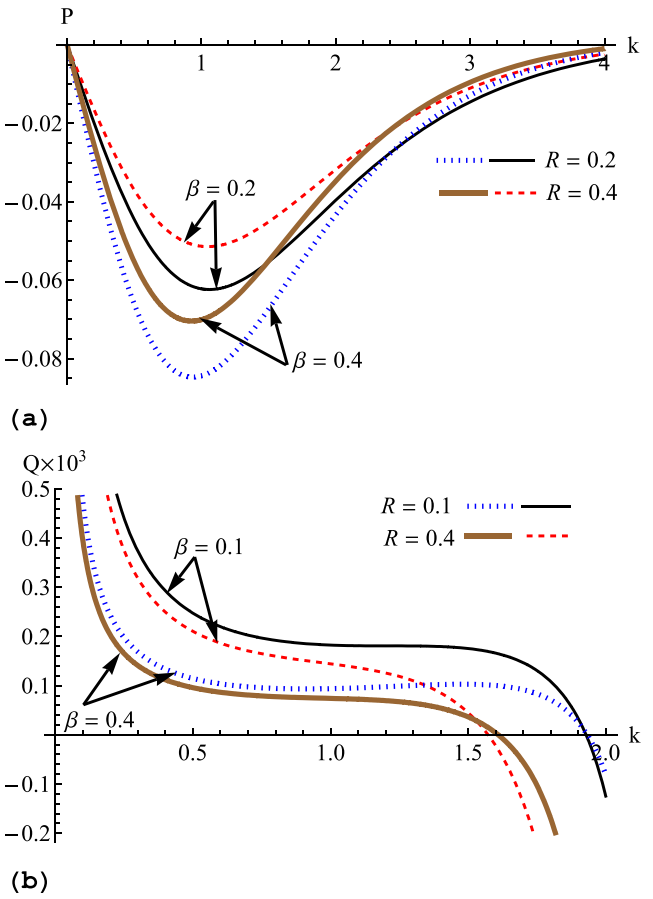

FIG. 2. Variation of the dispersion [nonlinear] coefficient, P [Q] in panel (a) [(b)], respectively, against k and β changes. The other parameters are selected as in Fig. 1.

geometries, the dependence of the total growth rate of the MI of nonlinear DA wave envelope, Γ that is presented by Eq (26), on R' and β, is investigated in Fig. 4(c). It clarifies that the highest growth rate is observed in the cylindrical geometry. Γ is an increasing function of R', though it reduces by increasing β. This figure proves that in the spherical geometry, the MI growth rate reaches a maximum value at $R' = R_c$ then it begins to decrease for $R' > R_c$, which coincides with what have been discussed above. Moreover, the variation of the explicit function, $f(R')$ appeared in Eqs. (26), versus R' in nonplanar geometry is presented in Fig. 4(d) showing that it has a similar behavior that illustrated in Fig. 4(c).

Now, to investigate the nature of the predicted rogue wave structures ψ_1 and ψ_2, we analyze the wave envelopes ψ_1 and ψ_2 and illustrate how the nonthermality parameter, β, changes the profiles of the fundamental/and the super rogue wave. The dependence of the fundamental/and the super rogue wave amplitude on β is introduced in Fig. 5. The latter shows a comparison between the first-order rational solution ψ_1 and the second-order rational solution ψ_2. It is noted that (i) ψ_2 has double structures compared with ψ_1, (ii) ψ_2 is more likely to break up a ship than ψ_1 since ψ_2 has more energy than of ψ_1 [cf. Fig. 6], and (iii) ψ_2 has higher amplitude than of ψ_1. Moreover, it is clear from Fig. 5 that the potential profile of ψ_2 becomes spiky (i.e., taller amplitude and narrower width) than of ψ_1.

To conclude, we have investigated the amplitude modulation of the nonplanar; cylindrical and spherical, DA

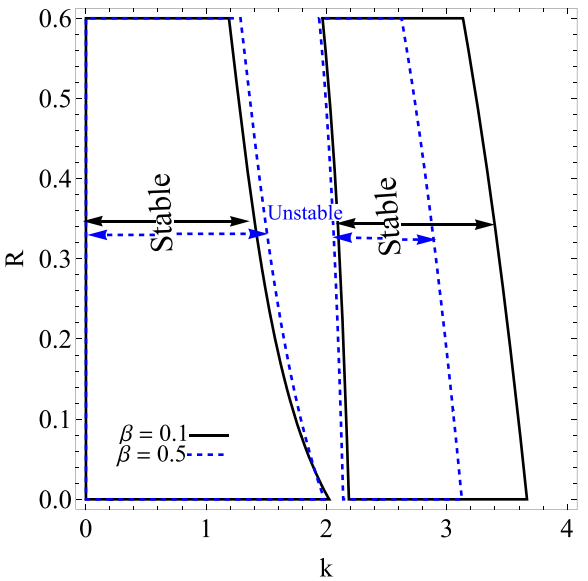

FIG. 3. The region plot of "PQ < 0" in the k-R domain is presented for different values of β (the regions of stable/unstable DA wave propagation are demonstrated). The other parameters are selected as in Fig. 1.

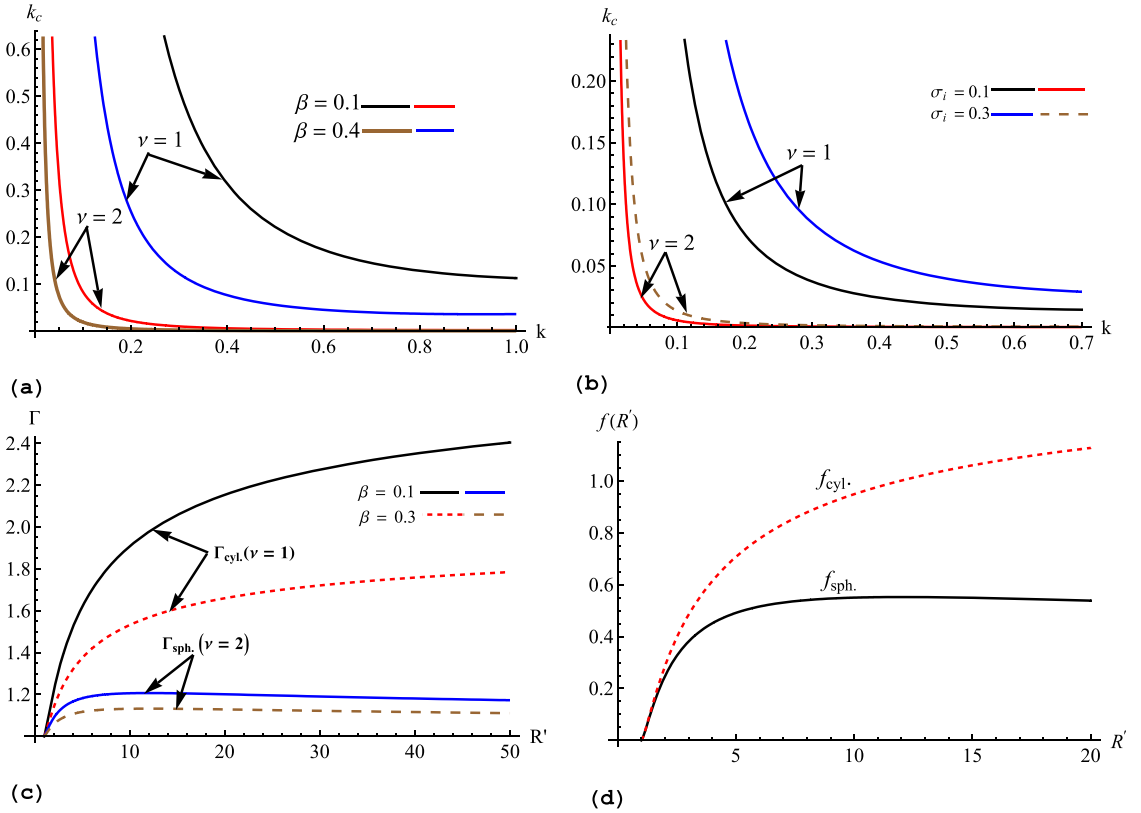

FIG. 4. Variation of the critical wave number, K_c, in (a) against the wave number, k, for different values of β in different geometries, and in (b) against k for different values of the ion to electron temperature parameter, σ_i, for $\sigma_d = 0.05$, $\mu_i = 6$, $\mu_e = 3$, $\tau = 0.02$, and $\beta = 0.6$, (c) variation of the growth rate, Γ against R' for different values of β in cylindrical and spherical geometries, and in (d) variation of $f(R')$ against R' in different geometries.

envelope solitary waves in an unmagnetized SCDP consisting of negative dust grains, Maxwellian electrons and nonthermal ions. A modified NLSE is derived for the wave amplitude modulation. It is found that the nature of the wave instabilities is significantly modified by changes in the nonthermality (polarization), β (R) parameter. This allows us to determine the MI domains of DA waves. The possible rational fundamental/super rogue wave solutions are also

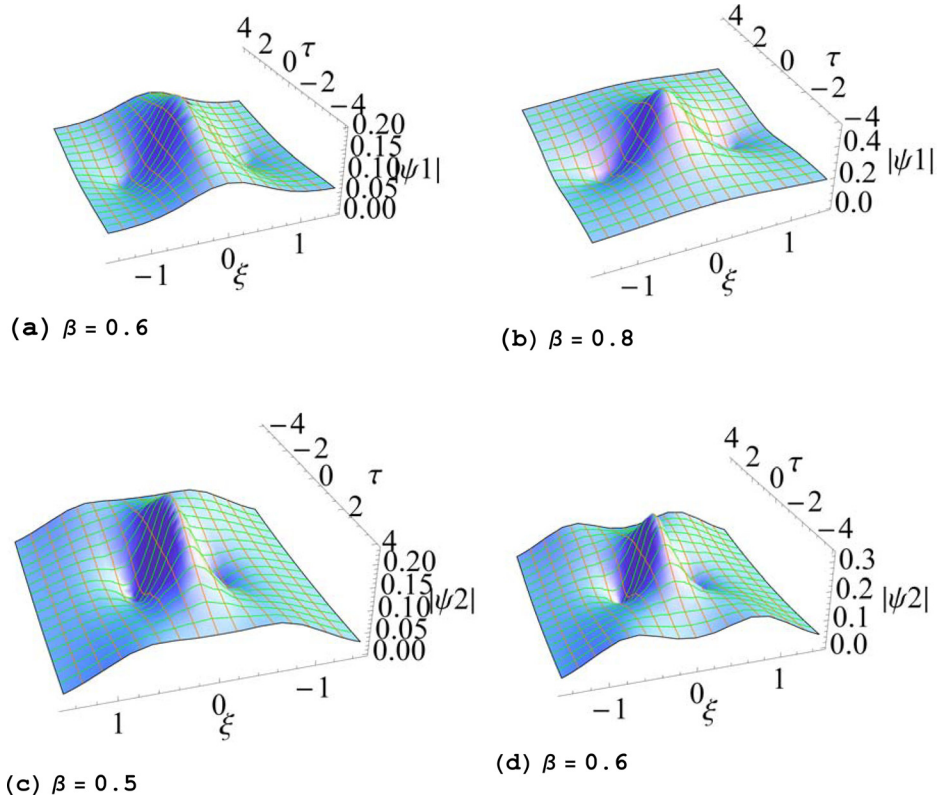

FIG. 5. Profiles of the first- and second-order rational solutions, ψ_1 and ψ_2, are presented, respectively. Variation of the fundamental rogue wave amplitude in $(\xi - \tau)$ space for different values of β are shown in panels (a) and (b) and the super rogue wave amplitude in panels (c) and (d) for $\sigma_i = 0.0375$, $\sigma_d = 0.01$, $\mu_i = 2.33$, $\mu_e = 1.33$, and $\tau = 0.025$.

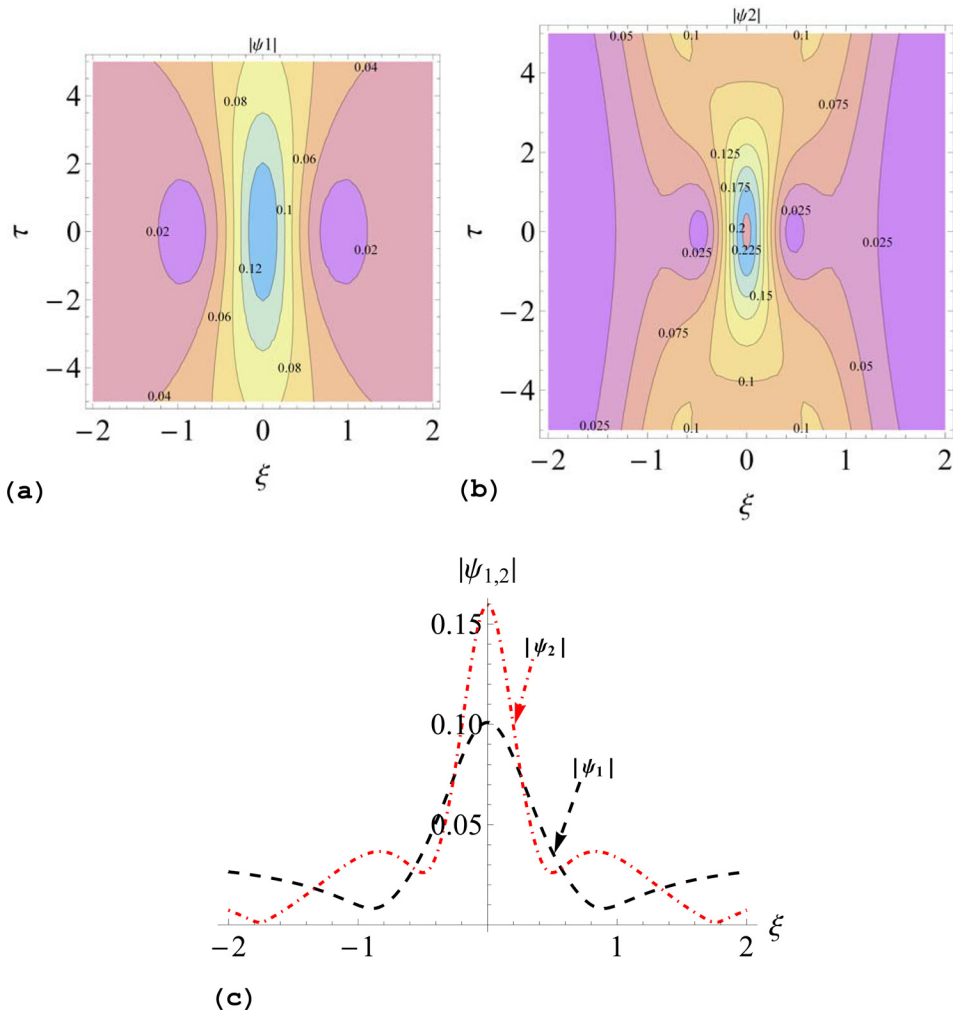

FIG. 6. Contour plot of the solutions presented in Fig. 5 along ξ and τ are introduced in (a), (b), and (c). The values beside the curves refers to the magnitude of $|\psi_1|$ and $|\psi_2|$. The selected physical parameters are the same as in Fig. 5 with R = 0.3.

investigated. It is found that the ion nonthermality parameter affects strongly on the characteristics of these rogue wave structures. The influence of the relevant physical parameters (nonthermality, polarization effect and the ion-to-electron temperature ratio) on the DA wave dynamics has been traced by observing the effect of parameters β, R and σ_i (respectively) on

(a) The angular frequency, ω, and the group velocity, λ.
(b) The dispersion coefficient, P, and the nonlinear coefficient, Q.
(c) The instability domain for the DA envelope solitary waves and the critical wave number K_c.

The critical wave number threshold, K_c, which indicates where the instability sets in, has been calculated in the nonplanar geometries. Also, there exists a MI period for the cylindrical and spherical envelope excitations, which does not exist in the one-dimensional planar case. During the unstable period, the MI growth rate is always an increasing function of R' in the cylindrical geometry, but not in the spherical geometry. This suggests that the spherical waves are more structurally stable to perturbations than the cylindrical waves. As the used numerical physical parameter values are inspired from recent experimental data,[23,24,26,49] we believe that the present results are helpful to existing and forthcoming experimental and space observations, where nonthermal SCDP is present.[48]

APPENDIX: THE EXPLICIT EXPRESSIONS OF THE COEFFICIENTS MENTIONED IN EQS. (10, 11, AND 14)

$$N_1 = -\left[\frac{\mu_e\sigma_i^2}{2} - \mu_i\left(\frac{1}{2}+\beta\right)\right] - \alpha_1\frac{N_2}{N_3},$$

$$N_2 = 2\omega\left\{\frac{-\omega}{k}\left[\frac{\mu_e\sigma_i^2}{2} - \mu_i\left(\frac{1}{2}+\beta\right)\right] - \frac{\alpha_n^2\omega}{k}\right\} + 2k\sigma_d\mu_d\left[\frac{\mu_e\sigma_i^2}{2} - \mu_i\left(\frac{1}{2}+\beta\right)\right] - \frac{\alpha_n^2\omega^2}{k} + \alpha_n^2 k\sigma_d\mu_d + \frac{kR}{2}(1-\beta),$$

$$N_3 = \frac{2\omega^2\alpha_1}{k} - 2k(1-R) - 2k\sigma_d\mu_d\alpha_1, \quad N_{23} = \frac{N_2}{N_3},$$

$$N_4 = \frac{\omega}{k}\left(N_1 - \alpha_n^2\right),$$

$$N_5 = \left(\mu_i(1+2\beta) - \mu_e\sigma_i^2\right) - \left(\mu_e + \mu_i(1-\beta)\right)\frac{N_7}{N_8},$$

$$N_6 = \frac{-2\alpha_n^2\omega}{k} + \lambda N_5,$$

$$N_7 = -\frac{\alpha_n^2\omega^2}{k^2} + \frac{R}{2}(1-\beta) + \alpha_n^2\sigma_d\mu_d - \frac{2\alpha_n^2\omega\lambda}{k} + \left(\lambda^2 - \sigma_d\mu_d\right)\left(\mu_i(1+2\beta) - \mu_e\sigma_i^2\right),$$

$$N_8 = \left(\lambda^2 - \sigma_d\mu_d\right)\left(\mu_e + \mu_i(1-\beta)\right) - (1-R), \quad N_{78} = \frac{N_7}{N_8},$$

$$\alpha_1 = 4k^2 + \mu_e\sigma_i + \mu_i(1-\beta), \quad a_1 = \lambda\tau\alpha_n\left(\lambda - \frac{\omega}{k}\right),$$

$$a_2 = \lambda\tau\left[2k\lambda - \left(-\frac{\alpha_n\lambda}{k} + \frac{\alpha_n\omega}{k^2} + 2\omega\right)\right],$$

$$a_3 = -2k\omega\xi + \alpha_n\lambda\xi - \frac{\alpha_n\omega\xi}{k} + k\xi\left(-\frac{\alpha_n\lambda}{k} + \frac{\alpha_n\omega}{k^2} + 2\omega\right),$$

$$a_4 = -\lambda\tau\alpha_n[k(2N_6 + N_4) + \omega(2N_5 + N_1)],$$

$$a_5 = \frac{\xi}{\lambda\tau}\left[-k^2 - \mu_e\sigma_i - \alpha_n + \mu_i(\beta - 1)\right],$$

$$a_6 = \left(\frac{2N_7}{N_8} + \frac{N_2}{N_3}\right)\left(-\mu_e\sigma_i^2 + \mu_i\right) - \frac{\mu_e\sigma_i^3}{2} - \frac{\mu_i}{2}(1+3\beta),$$

$$a_7 = \lambda\left(\frac{-\alpha_n\lambda}{k} + \frac{\alpha_n\omega}{k^2} + 2\omega\right) - 2k\sigma_d\mu_d,$$

$$a_8 = \frac{\alpha_n\omega\lambda}{k} + 1 - R - \alpha_n\sigma_d\mu_d,$$

$$a_9 = -\alpha_n\omega(2N_6 + N_4) + k\alpha_n\sigma_d\mu_d(2N_5 + N_1) - \alpha_n^3 k\sigma_d\mu_d + \frac{kR}{2}\left[(1-\beta)\left(2\frac{N_7}{N_8} + \frac{N_2}{N_3}\right) - \frac{\beta}{2} + \frac{(\beta^2-1)}{4}\right].$$

[1]P. K. Shukla and A. A. Mamun, *Introduction to Dusty Plasma Physics* (IOP, Bristol, 2002).
[2]N. N. Rao, P. K. Shukla, and M. Y. Yu, Planet. Space Sci. **38**, 543 (1990).
[3]A. Barkan, R. Merlino, and N. D'Angelo, Phys. Plasmas **2**, 3563 (1995).
[4]W. F. El-Taibany, I. Kourakis, and M. Wadati, Plasma Phys. Controlled Fusion **50**, 074003 (2008).
[5]M. R. Amin, G. E. Morfill, and P. K. Shukla, Phys. Rev. E **58**, 6517 (1998).
[6]I. Kourakis and P. K. Shukla, Phys. Plasmas **10**, 3459 (2003).
[7]X. Jukui and T. Rongan, Phys. Scr. **67**, 74 (2003).
[8]R.-A. Tang and J.-K. Xue, Phys. Plasmas **10**, 3800 (2003).
[9]A. A. Mamun and P. K. Shukla, Phys. Lett. A **290**, 173 (2001).
[10]A. A. Mamun and P. K. Shukla, Phys. Plasmas **9**, 1468 (2002).
[11]J. K. Xue, Phys. Plasmas **10**, 3430 (2003).
[12]J. R. Franz, P. M. Kintner, and J. S. Pickett, Geophys. Res. Lett. **25**, 1277, doi:10.1029/98GL50870 (1998).
[13]I. Kourakis and P. K. Shukla, IEEE Trans. Plasma Sci **32**, 5743 (2004); Phys Scr. **69**, 316 (2004).
[14]Y. Wang, X. Jiang, C. Guo, and Z. Zhou, Phys. Lett. A **375**, 832 (2011).
[15]S. K. El-Labany, W. F. El-Taibany, and M. Mahmoud, Phys. Scr. **87**, 055502 (2013).
[16]J. R. Asbridge, S. J. Bame, and I. B. Strong, J. Geophys. Res. **73**, 5777 (1968); R. Lundin *et al.*, Nature (London) **341**, 609 (1989); Y. Futaana *et al.*, J. Geophys. Res. **108**, 151 (2003).
[17]A. A. Mamun, R. A. Cairns, and P. K. Shukla, Phys. Plasmas **3**, 2610 (1996); H. Asgari, S. V. Muniandy, and C. S. Wong, *ibid.* **20**, 023705 (2013).
[18]W. F. El-Taibany and R. Sabry, Phys. Plasmas **12**, 082302 (2005); W. F. El-Taibany, A. Mushtaq, W. M. Moslem, and M. Wadati, *ibid.* **17**, 034501 (2010).
[19]A. P. Misra and A. R. Chowdhury, Eur. Phys. J. D **39**, 49 (2006); W. F. El-Taibany and I. Kourakis, Phys. Plasmas **13**, 062302 (2006).
[20]I. Ikezi, Phys. Fluids **29**, 1764 (1986).
[21]M. Rosenberg and G. Kalman, Phys. Rev. E **56**, 7166 (1997); P. K. Kaw and A. Sen, Phys. Plasmas **5**, 3552 (1998); M. S. Murillo, *ibid.* **5**, 3116 (1998); M. S. Murillo, *ibid.* **7**, 33 (2000); B. M. Veeresha, S. K. Tiwari, A. Sen, P. K. Kaw, and A. Das, Phys. Rev. E **81**, 036407 (2010).
[22]A. A. Mamun and P. K. Shukla, New J. Phys. **11**, 103022 (2009); H. R. Pakzad and K. Javidan, Pramana J. Phys. **73**, 913 (2009); M. S. Rahman and A. A. Mamun, Phys. Plasmas **18**, 123702 (2011); M. S. Rahman, B. Shikha, and A. A. Mamun, J Plasma Phys. **79**, 249 (2013).
[23]A. A. Mamun, K. S. Ashrafi, and P. K. Shukla, Phy. Rev. E **82**, 026405 (2010); H. Alinejad and A. A. Mamun, Phys Plasmas **18**, 073706 (2011); M. Asaduzzaman and A. A. Mamun, Phys. Rev. E **86**, 016409 (2012); K. S. Ashrafi, A. A. Mamun, and P. K. Shukla, J. Plasma Phys. **80**, 1 (2014).
[24]S. K. El-Labany, W. F. El-Taibany, E. F. El-Shamy, A. El-Depsy, and N. A. Zedan, Phys. Plasmas **19**, 103708 (2012); S. K. El-Labany, E. F. El-Shamy, W. F. El-Taibany, and N. A. Zedan, Chin Phys. B **24**, 035201 (2015).
[25]K. S. Ashrafi, A. A. Mamun, and P. K. Shukla, EPL **92**(1), 15004 (2010); S. Islam, A. A. Mamun, and A. Mannan, J. Plasma Phys. **78**, 629 (2012).
[26]S. K. El-Labany, W. F. El-Taibany, E. F. El-Shamy, and N. A. Zedan, Phys. Plasmas **21**, 123710 (2014).
[27]C. Cui and J. Goree, IEEE Trans. Plasma Sci. **22**, 151 (1992); J. Goree, Plasma Sources Sci. Technol. **3**, 400 (1994); S. K. El-Labany, W. F. El-Taibany, N. A. El-Bedwehy, and M. M. El-Fayoumy, Eur. Phys. J. D **64**, 375 (2011).
[28]R. A. Cairns, A. A. Mamun, R. Bingham, R. Dendy, R. Bostrom, C. M. C. Nairns, and P. K. Shukla, Geophys. Res. Lett. **22**, 2709, doi:10.1029/95GL02781 (1995).
[29]S. Hamaguchi and R. T. Farouki, Phys. Rev. E **49**, 4430 (1994); Phys. Plasmas **1**, 2110 (1994); S. A. Khrapak, A. V. IvIev, V. V. Yaroshenko, and G. E. Morfill, Phys. Rev. Lett. **102**, 245004 (2009).
[30]S. Ichimaru, H. Iyetomi, and S. Tanaka, Phys. Rep.**149**, 91 (1987).
[31]A. A. Mamun and R. A. Cairns, Phys. Rev. E **79**, 055401(R) (2009).
[32]M. A. Berkovsky, Phys. Lett. A **166**, 365 (1992).
[33]W. L. Slattery, G. D. Doolen, and H. E. DeWitt, Phys. Rev. A **21**, 2087 (1980).
[34]A. A. Mamun, P. K. Shukla, and T. Farid, Phys. Plasmas **7**, 2329 (2000).
[35]T. Taniuti and N. Yajima, J. Math. Phys. **10**, 1369 (1969); N. Asano, T. Taniuti, and N. Yajima, *ibid.* **10**, 2020 (1969); T. Kawahara, J. Phys. Soc. Jpn. **35**, 1537 (1973); M. Y. Yu, P. K. Shukla, and S. Bujarbarua, Phys. Fluids **23**, 2146 (1980); P. K. Shukla and A. A. Mamun, New J. Phys. **5**, 17 (2003).
[36]X. Jukui, Phys. Plasmas **11**, 1860 (2004).
[37]A. Ankiewicz, P. A. Clarkson, and N. Akhmediev, J. Phys. A: Math. Theor. **43**, 122002 (2010).
[38]N. Akhmediev, A. Ankiewicz, and M. Taki, Phys. Lett. A **373**, 675 (2009); N. Akhmediev, J. M. Soto-Crespo, and A. Ankiewicz, *ibid.* **373**, 2137 (2009); A. Ankiewicz, N. Devine, and N. Akhmediev, *ibid.* **373**, 3997 (2009).
[39]Z. Yan, V. V. Konotop, and N. Akhmediev, Phys. Rev. E **82**, 036610 (2010).
[40]N. N. Akhmediev, V. M. Eleonskii, and N. E. Kulagin, Sov. Phys. JETP **62**, 894 (1985); N. N. Akhmediev and A. Ankiewicz, *Solitons: Nonlinear Pulses and Beams*, Optical and Quantum Electronics, Vol. 5 (Chapman & Hall, London, 1997).
[41]N. Akhmediev, A. Ankiewicz, and J. M. Soto-Crespo, Phys. Rev. E **80**, 026601 (2009).
[42]Ata-ur-Rahman, M. Mc Kerr, W. F. El-Taibany, I. Kourakis, and A. Qamar, Phys. Plasmas **22**, 022305 (2015).
[43]D. H. Peregrine, J. Aust. Math. Soc. Ser. B, Appl. Math. **25**, 16 (1983).
[44]A. Chabchoub, N. Hoffmann, M. Onorato, and N. Akhmediev, Phys. Rev. X **2**, 011015 (2012).
[45]S. Guo, L. Mei, and A. Sun, Ann. Phys. **332**, 38 (2012).
[46]X. Jukui and H. Lang, Phys. Plasmas **10**, 339 (2003).
[47]I. Kourakis, M. Mc Kerr, and I. K. A. Q. Ata-ur-Rahman, J. Plasma Physics **79**, 1089 (2013).
[48]N. S. Saini and I. Kourakis, Phys. Plasmas **15**, 123701 (2008).
[49]P. Bandyopadhyay, G. Prasad, A. Sen, and P. K. Kaw, Phys. Rev. Lett.**101**, 065006 (2008).